

Article

Analysis of Ion-Exchanged ZSM-5, BEA, and SSZ-13 Zeolite Trapping Materials under Realistic Exhaust Conditions

Todd J. Toops^{1,*}, Andrew J. Binder^{1,†}, Pranaw Kunal¹, Eleni A. Kyriakidou²  and Jae-Soon Choi^{1,‡} 

¹ National Transportation Research Center, Oak Ridge National Laboratory, Knoxville, TN 37932, USA; binder.andrewj@gmail.com (A.J.B.); kunalp@ornl.gov (P.K.); jaesoonchoi@lgchem.com (J.-S.C.)

² Department of Chemical and Biological Engineering, The State University of New York, Buffalo, NY 14260, USA; eleniky@buffalo.edu

* Correspondence: toopstj@ornl.gov

† Currently at Galbraith Laboratories Inc.

‡ Currently at LG Chem Ltd.

Abstract: An industry-defined evaluation protocol was used to evaluate the hydrocarbon trapping (HCT) and passive NO_x adsorption (PNA) potential for BEA, ZSM-5, and SSZ-13 zeolites with ion-exchanged Pd or Ag. All materials underwent 700 °C degreening prior to exposure to an industry-derived protocol gas stream, which included NO_x, ethylene, toluene, and decane as measured trapping species as well as common exhaust gasses CO, H₂O, O₂, CO₂, and H₂. Evaluation showed that BEA and ZSM-5 zeolites were effective at trapping hydrocarbons (HCs), as saturation was not achieved after 30 min of exposure. SSZ-13 also stored HCs but was only able to adsorb 20–25% compared to BEA and ZSM-5. The presence of Ag or Pd did not impact the overall HC uptake, particularly in the first three minutes. Pd/zeolites had significantly lower THC release temperature, and it aided in the conversion of the released HCs; Ag only had a moderate effect in both areas. With respect to NO_x adsorption, the level of uptake was much lower than HCs on all samples, and Ag or Pd was necessary with Pd being notably more effective. Additionally, only Pd/ZSM-5 and Pd/SSZ-13 continue to store a portion of the NO_x above 200 °C, which is critical for downstream selective catalytic NO_x reduction (SCR). Hydrothermal aging (800 °C for 50 h) of a subset of the samples were performed: BEA, Pd/BEA, ZSM-5, Pd/ZSM-5, and Pd/SSZ-13. There was a minimal effect on the HC storage, ~10% reduction in capacity with no effect on release temperature; however, only Pd/SSZ-13 showed significant NO_x storage after aging.



Citation: Toops, T.J.; Binder, A.J.; Kunal, P.; Kyriakidou, E.A.; Choi, J.-S. Analysis of Ion-Exchanged ZSM-5, BEA, and SSZ-13 Zeolite Trapping Materials under Realistic Exhaust Conditions. *Catalysts* **2021**, *11*, 449. <https://doi.org/10.3390/catal11040449>

Academic Editor: Philippe Vernoux

Received: 4 March 2021

Accepted: 26 March 2021

Published: 31 March 2021

Publisher's Note: MDPI stays neutral with regard to jurisdictional claims in published maps and institutional affiliations.



Copyright: © 2021 by the authors. Licensee MDPI, Basel, Switzerland. This article is an open access article distributed under the terms and conditions of the Creative Commons Attribution (CC BY) license (<https://creativecommons.org/licenses/by/4.0/>).

Keywords: hydrocarbon trap (HCT); passive NO_x adsorber (PNA); silver; palladium; zeolite

1. Introduction

Since the 1970s automotive emissions control has been a continual challenge due to increasing understanding of the hazards of pollutants and subsequently increasing regulatory efforts to lower harmful emissions. Initially, much of the lean-burn automotive emissions reduction was handled through emissions-conscious engine design and the use of a diesel oxidation catalyst (DOC) [1–7]. However, modern lean-burn emissions control requires a complex approach involving a series of specialized materials [8–14] to manage the wide variety of pollutants and exhaust conditions due to the increasingly strict emissions standards. These include diesel particulate filters (DPF) and selective catalytic NO_x reduction catalysts (SCR), in addition to the DOC.

This emissions control system requires a minimum exhaust temperature to become fully effective, and thus, a significant percentage of the overall emissions occur in the first 1–2 min after starting the engine [15–17]. Additionally, improved engine efficiency results in cooler exhaust [18–21], such that under low load operation the exhaust and catalyst temperatures could temporarily decrease to the point the catalysts are not active in the

emissions control system [20]. In most cases temperatures less than 200 °C would be considered a significant challenge for emissions control catalysts [20]. This temperature is typical for DOCs to be able to convert greater than 90% of the exhaust CO and total hydrocarbons (THCs), and above this temperature urea can be injected, which will hydrolyze to NH₃ and is used to reduce NO_x over the SCR. Development of a solution to these low temperature emissions control challenges is crucial to meeting future emissions requirements [21,22].

One frequently proposed approach to reducing low temperature emissions is the introduction of trapping materials within the emissions control system that would be capable of adsorbing HC and NO_x until the catalysts have warmed up enough to become reactive [16,23–27]. Development of effective trapping materials often focuses on three primary factors: (i) a significant adsorption capacity at low temperatures (<200 °C), (ii) a desorption temperature compatible with emissions control active windows (greater than 200 °C), and (iii) suitable durability against hydrothermal aging. With these factors in mind, a variety of zeolites have shown great promise in studies for the adsorption of common exhaust components such as CO, light and heavy HCs [26–30], and NO_x species [31–34]. Unfortunately, many fundamental studies are often conducted in simplified gas streams which result in many questions as to their applicability to automotive systems which can include high concentrations of water and CO₂, multiple types of HC species, NO_x, CO, and high space velocity. On the other end of the research spectrum, industrially relevant studies are performed with full exhaust gas from engines [35–37]. These realistic evaluations show how the materials would work in the application, but the hundreds of different HCs in the exhaust make it difficult to track the individual components. Thus, evaluation of potential trapping materials under complex, yet manageable flow constituents, is necessary to prove feasibility, highlight challenges, and identify which family of exhaust components are most challenging.

With that in mind, we present an evaluation of nine zeolite-based trapping materials utilizing a flow reactor protocol developed by a collaboration of industry, national laboratories, and academic researchers [38,39] to mimic realistic lean-burn automotive exhaust. As described in detail below, this protocol includes the opportunity to simultaneously trap CO, NO_x, and three HCs representative of those found in automotive exhaust: ethylene (short-chain alkenes), toluene (aromatics), and decane (long-chain alkanes). ZSM-5, BEA, and SSZ-13 zeolites and two ion-exchange metals, Pd or Ag, were chosen for this study based on previous reports of high storage efficiency and suitable release temperatures [40–46]. The representative structure of each of these zeolites are shown in Figure 1. Evaluation of both the storage and release characteristics of these materials was performed to elucidate the attributes of each material.

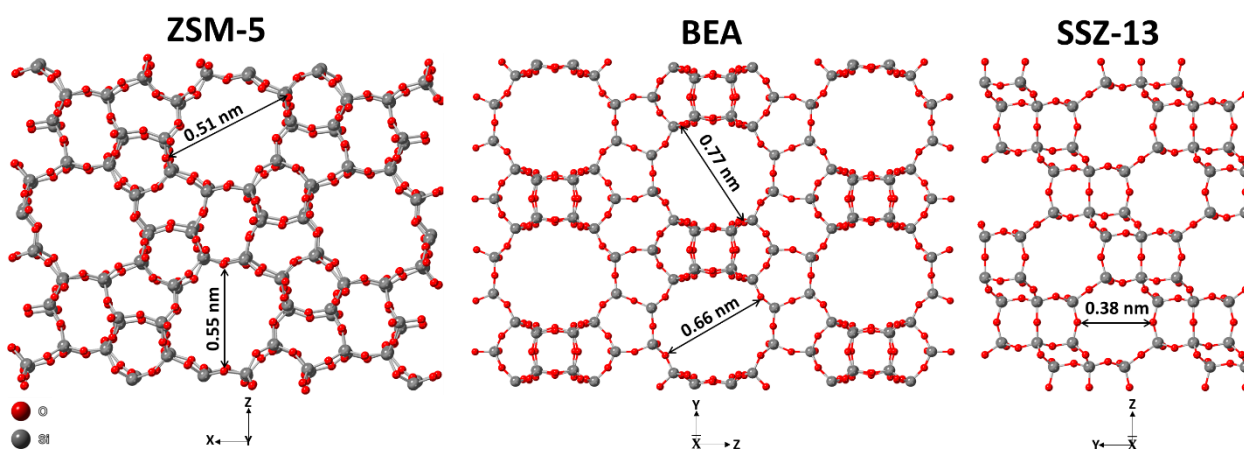


Figure 1. Representation of zeolite structures deployed in this study.

2. Results and Discussion

2.1. Hydrocarbon Trapping

An ideal hydrocarbon trap (HCT) would have high storage below 200 °C and release HCs above 200 °C where a DOC could oxidize them to CO₂ and H₂O. To understand how the evaluated samples meet these HCT criteria, a systematic analysis routine was employed. Figure 2 shows a characteristic storage and release profile for each of the three trials on Pd/ZSM-5. The difference between the reactor effluent and the bypass gas concentration indicates a large amount of storage on this sample, and we have analyzed this storage in 2 parts. The first portion is 3 min and is related to how much storage would be expected under a typical startup condition [47,48]. It is represented by the blue shading with white dots (■) in Figure 2a and is quantified in Figure 2b. The second portion up to 30 min is related to total storage capacity (white with blue dots, ■, in Figure 2a,b), but as can be seen here, the sample was not fully saturated as the bypass concentration was not reached. After the 30-min storage, the reactant gases are turned off, and the sample is quickly heated to 600 °C. During this portion of the experiment the HCs desorb from the sample, and some of them react to form CO and CO₂. As suggested by the protocol [38,39], the release profile is described by three characteristic temperatures. The first is the temperature of 10% release (T10), i.e., the temperature where 10% of the observed desorbed HCs were released. This is also shown in Figure 2a with a dark blue shading (■) beginning at 30 min (0% release) and continuing to ~33 min (10% release); the temperature is also indicated with a dark blue arrow. Figure 2c indicates this value with the dark blue (■) portion of the bar. The next segment indicates the temperature of 50% release (T50). In Figure 2a this is represented with the medium blue shading (■) that reaches from 10% to 50% and the temperature is indicated with medium blue arrow and by the second section of the bar in Figure 2c (■). The next segment of interest is for 90% release of the HCs, which is represented by a light blue shading (■) for the 50–90% release in Figure 2a. The T90 is represented by a light blue arrow in Figure 2a and the top segment of the bar in Figure 2c (■).

This approach is used for each of the samples evaluated, and the full bar charts for both HC storage values (mmols C₁/g_{cat}) and release temperatures for the degreened samples are shown in Figure 3 with the values listed in Table 1. All the BEA and ZSM-5 samples have similar uptake during the first 3 min with an uptake of 0.9–1.0 mmols C₁/g_{cat}. The SSZ-13 samples have notably less uptake with only 0.6–0.7 mmols C₁/g_{cat} occurring in the first 3 min. After 30 min the BEA samples store between 4.8 and 5.1 mmols C₁/g_{cat} while the ZSM-5 samples have slightly less uptake of 4.3–5.0 mmols C₁/g_{cat}. The SSZ-13 samples reach saturation well before 30 min and only uptake a total of 0.9–1.0 mmols C₁/g_{cat} after 30 min. These results clearly indicate that the larger pore structures associated with BEA (0.7–0.8 nm) and ZSM-5 (0.5–0.6 nm) allow more uptake of the HCs studied here compared to SSZ-13 (~0.4 nm), which has smaller pores [49,50]. An additional observation is that the presence of Ag or Pd does not generally result in higher uptake of the HCs in any of these samples. The one exception to this observation is that Ag/ZSM-5 uptakes 5.0 mmols C₁/g_{cat} compared to 4.3–4.4 for the other ZSM-5 samples. Enhanced uptake capacity in the presence of Ag has been reported elsewhere [27,40,51], so it is interesting that we do not observe it in this study. A likely explanation is the large size and concentration of the decane molecule used here overwhelming the adsorption sites and zeolite pores; most prior work reporting these benefits of metals focused on shorter hydrocarbon lengths [27,40,51,52].

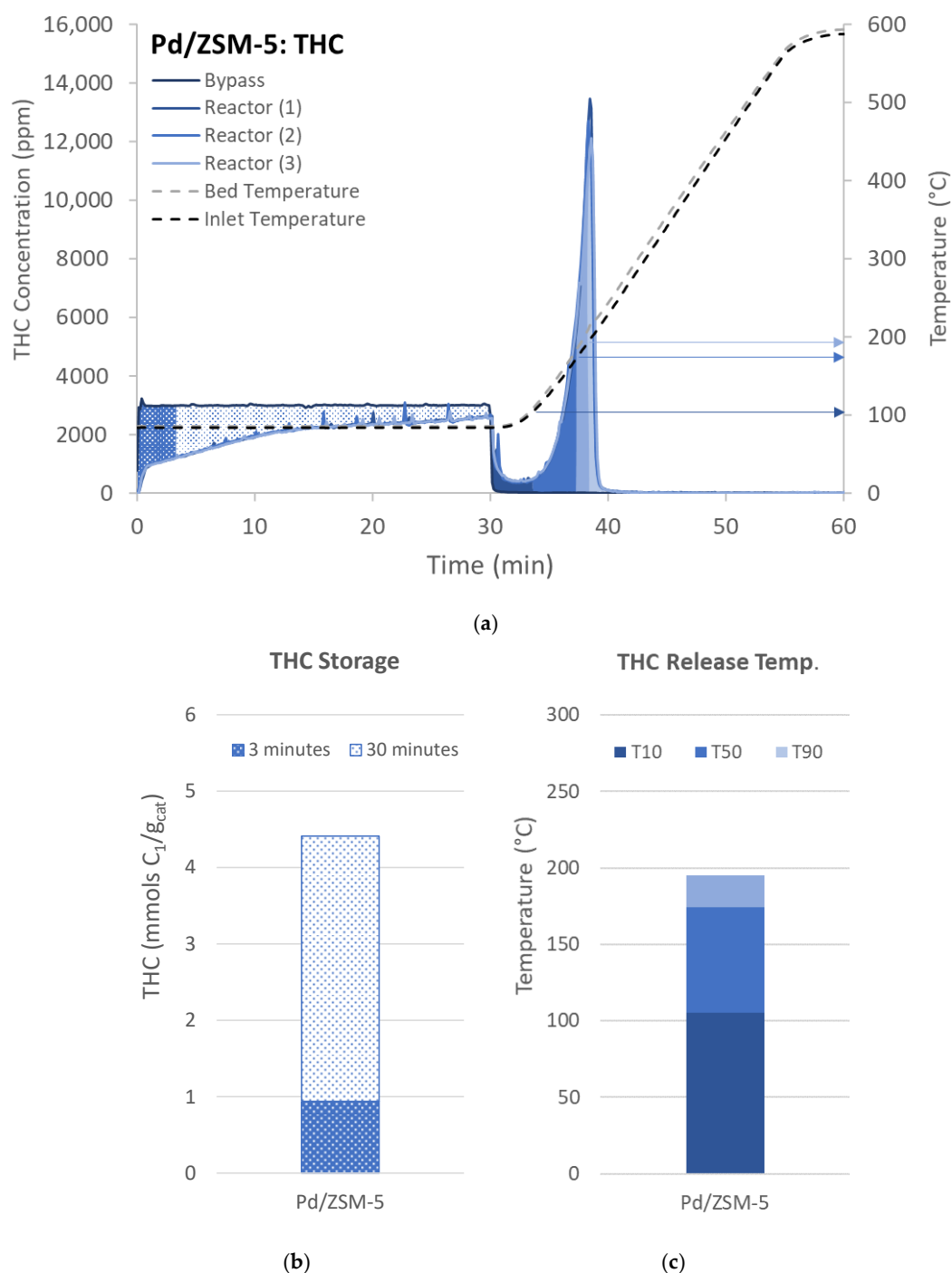


Figure 2. (a) THC concentration for each of the three reactor evaluations throughout the 60 min experiment. The shading represents 3 (■) and 30 (▨) minutes of adsorption during uptake and the zones/temperatures associated with 10% (T10, ■), 50% (T50, ■), or 90% (T90, ■) of THC released during desorption, which are also indicated with arrows. These characteristics are then represented by bar charts for both (b) adsorption and (c) desorption.

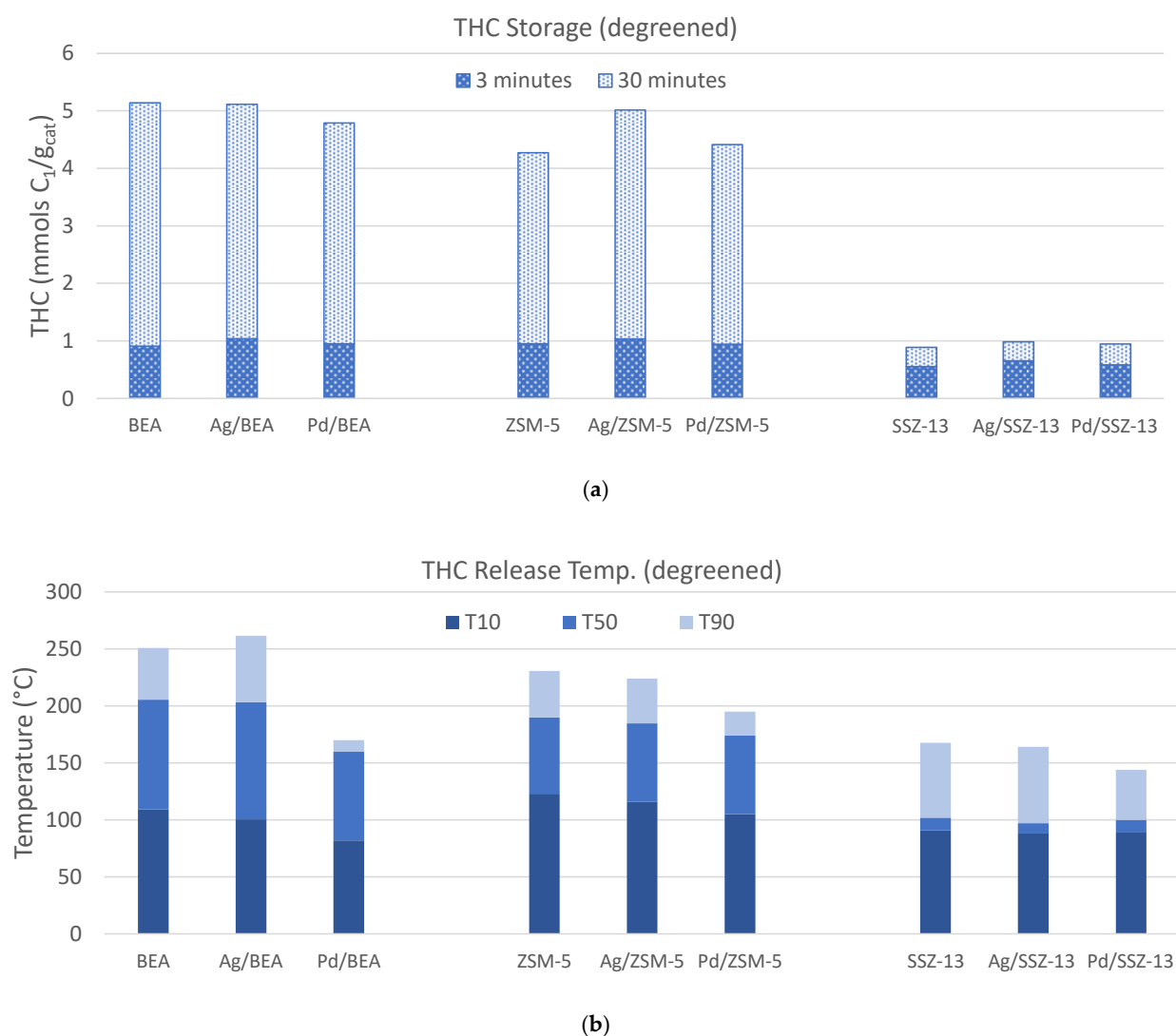


Figure 3. (a) THC adsorption after 3 (■) and 30 (▨) minutes for each of the materials studied. (b) The temperature where 10% (T10, ■), 50% (T50, ■), or 90% (T90, ■) of THC is released.

Table 1. THC storage values (mmol/ g_{cat}) for ion-exchanged zeolites during lean trapping evaluation after 3 and 30 min; THCs are reported on a C_1 basis. The total amount of observed THC released during the first 15 min of the ramp, and the temperature where 10% (T10), 50% (T50), or 90% (T90) of THC is released is also shown.

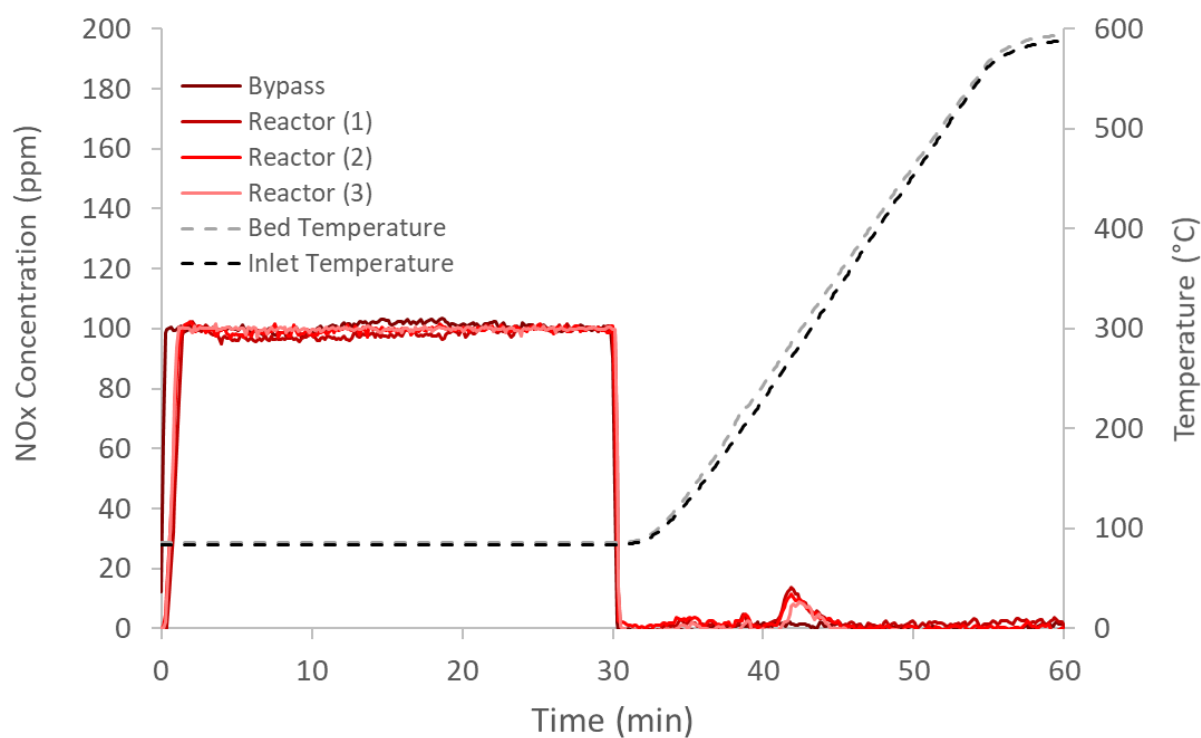
LTC-D (Storage) Degreened Zeolite	THC Storage (mmols C_1/g_{cat})		THC Release (mmols C_1/g_{cat}) 15 min	Release Temperature		
	3 min	30 min		T10 (°C)	T50 (°C)	T90 (°C)
BEA	0.9	5.1	5.2	109	205	251
Ag/BEA	1.0	5.1	4.5	101	203	262
Pd/BEA	1.0	4.8	2.0	82	160	170
ZSM-5	1.0	4.3	4.7	123	190	231
Ag/ZSM-5	1.0	5.0	5.0	116	185	224
Pd/ZSM-5	0.9	4.4	3.8	105	174	195
SSZ-13	0.6	0.9	1.0	91	102	168
Ag/SSZ-13	0.7	1.0	1.0	88	97	164
Pd/SSZ-13	0.6	0.9	0.8	89	100	144

At the end of the storage phase, a portion of the HCs is released, but most of them stay adsorbed until higher temperatures. The temperature of 10% release (T10) is shown in

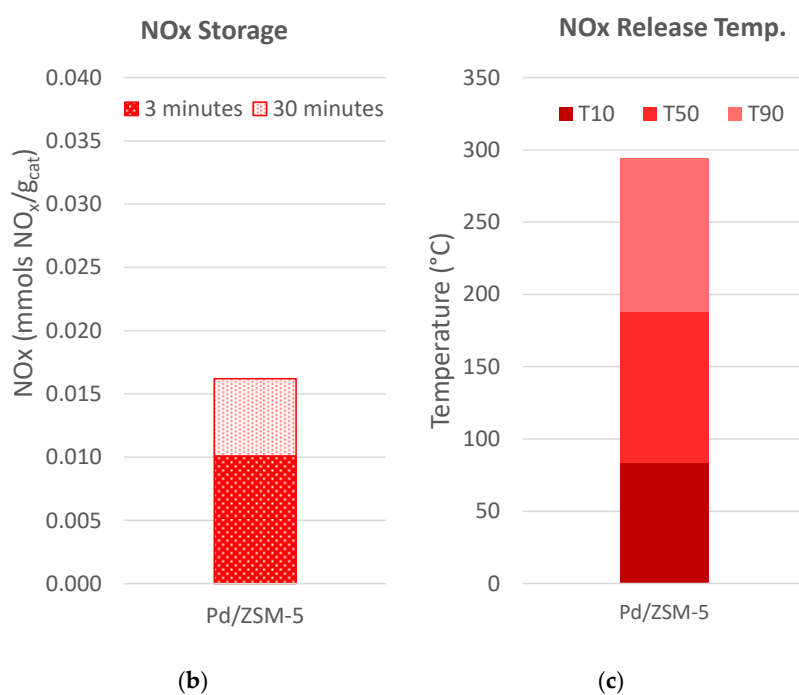
Figure 3 and listed in Table 1, and there are no distinct trends across the nine samples other than that the Pd/zeolites have the lowest T10. Comparing T50s and T90s, the Pd/zeolites continue to show lower release temperatures for the BEA and ZSM-5 samples. Since a small quantity of HCs are adsorbed on the SSZ-13 samples direct comparisons with BEA and ZSM-5 are difficult, but the trend of T90 being the lowest on the Pd sample is consistent. One of the confounding factors in evaluating the samples as we describe here, is that Pd is an excellent oxidation catalyst and the released HCs are readily oxidized over these zeolites in the presence of excess O₂ [40]. Thus, even though 90% of the HCs are released below the previously mentioned goal of 200 °C, the ability to convert the HCs directly on the HCT is a desirable feature. The released HC quantity is listed in Table 1, and in each Pd containing sample the released HC is less than the quantity stored at 30 min. This is most apparent in the Pd/BEA where nearly 60% of the released HC is converted. This feature could possibly allow for a smaller DOC, or at least less PGM content to balance the PGM being used in the HCT; this is the focus of a future study of ours. It should be noted that although Ag is not an excellent oxidation catalyst, it is expected to catalyze a portion of the stored HCs, and there is evidence of this in the Ag/BEA sample with 12% less HCs observed during the release compared to the uptake. Another key observation in the release temperatures is that both BEA and Ag/BEA release 50% of the HC above 200 °C, and thus many DOCs would be able to oxidize the HCs upon their release. ZSM-5 and Ag/ZSM-5 have similar stability, but their T50s are 190 and 185 °C, respectively, and thus not as desirable as the BEA samples. The SSZ-13 zeolites not only store less HCs, but they release nearly all of the HCs by 150 °C, and thus continue to show undesirable HCT properties.

2.2. NO Storage

As discussed above an ideal passive NO_x adsorber (PNA) would have high storage below 200 °C and release NO_x above 200 °C where a downstream SCR could be used in conjunction with ammonia from hydrolyzed urea. This hydrolysis occurs above 133 °C [53], and the SCR reactivity typically reaches 90% by 180 °C [54,55]. The same systematic analysis procedure described above in the HC section was also used with NO_x to understand how the evaluated samples meet the PNA criteria. Figure 4 shows a characteristic NO_x storage and desorption profile; Pd/ZSM-5 is shown here, which is the same sample and experiment shown in Figure 2. Notably less NO_x is adsorbed than HCs, but the adsorbed NO_x is more strongly bound and releases at higher temperatures. Similar to THC, the uptake is divided into two sections, 3 (■) and 30 (▣) minutes (Figure 4b), and the temperatures of 10%, 50% and 90% NO_x release are determined (Figure 4c). The data for all the samples are shown in Figure 5 with the specific values listed in Table 2. From these data two important observations are apparent. First, the Pd-zeolites are the only samples to have significant uptake, and second, only Pd/ZSM-5 and Pd/SSZ-13 maintains 50% of the NO_x above 150 °C; in fact, over 50% of the NO_x is still on Pd Pd/SSZ-13 at 224 °C. This finding is consistent with other reports of Pd/SSZ-13 being one of the best PNAs [56,57] and that NO storage only occurs on ion-exchanged Pd sites [41]. Neither catalyst closed the NO_x balance during release, suggesting there is some direct reduction in the stored NO_x from HCs. This typically yields some N₂O formation, but this reactor was not equipped with an analyzer that would allow N₂O to be measured accurately.



(a)



(b)

(c)

Figure 4. (a) NO_x concentration for each of the three reactor evaluations throughout the 60 min experiment. (b) NO_x adsorption after 3 (■) and 30 (▣) minutes for Pd ZSM-5, and (c) the temperature where 10% (T10, ■), 50% (T50, ■), or 90% (T90, ■) of the NO_x is released for PD/ZSM-5.

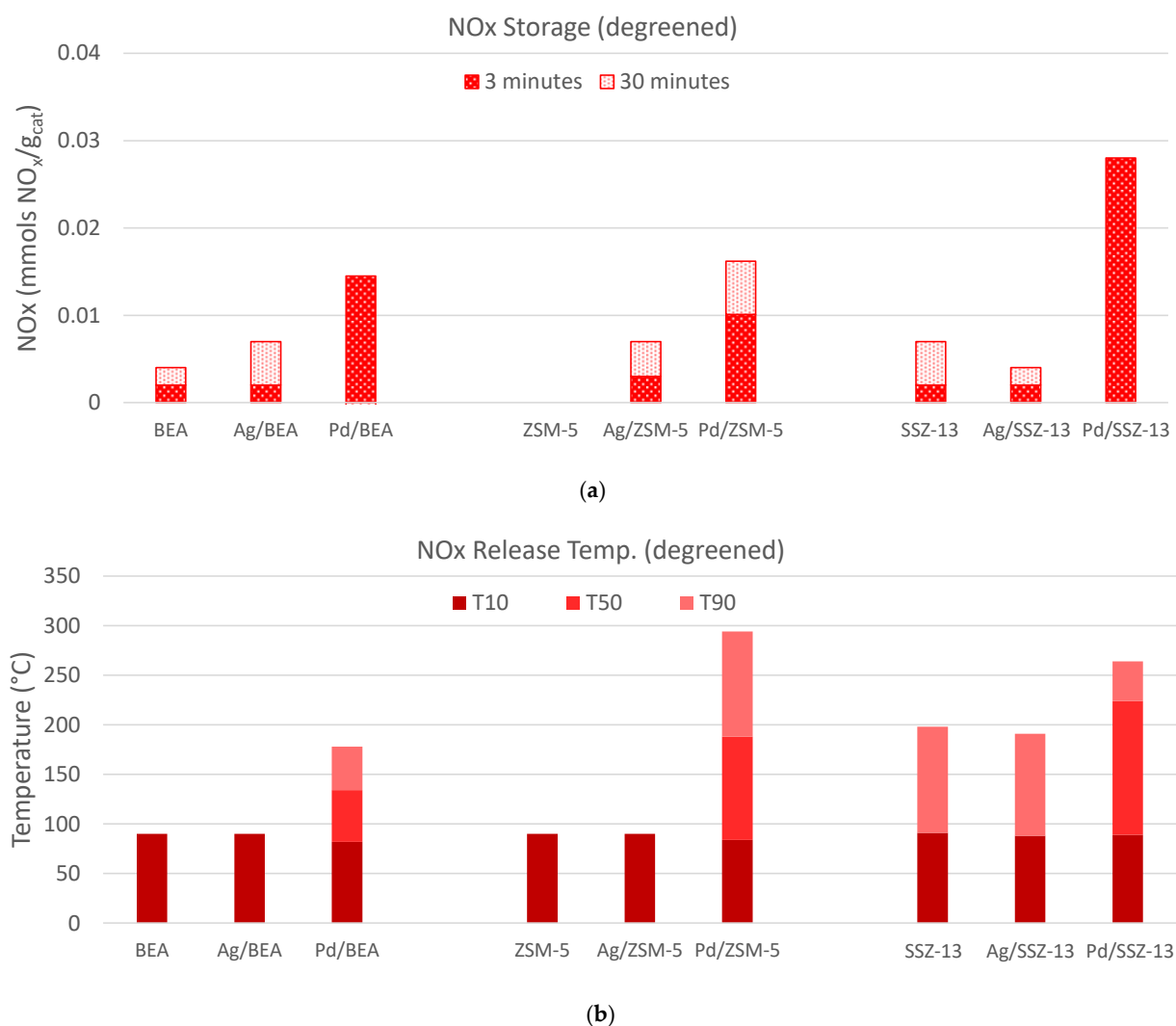


Figure 5. (a) NO_x adsorption after 3 (■) and 30 (▨) minutes for each of the materials studied. (b) The temperature where 10% (T10, ■), 50% (T50, ■), or 90% (T90, ■) of the NO_x is released.

Table 2. NO_x storage values (mmol/g_{cat}) for ion-exchanged zeolites during lean trapping evaluation after 3 and 30 min. The total amount of observed NO_x released during the first 15 min of the ramp, and the temperature where 10% (T10), 50% (T50), or 90% (T90) of NO_x is released is also shown.

LTC-D (Storage) Degreened Zeolite	NO _x Storage (mmols NO _x /g _{cat})		NO _x Release (mmols NO _x /g _{cat}) 15 min	Release Temperature		
	3 min	30 min		T10 (°C)	T50 (°C)	T90 (°C)
BEA	0.002	0.004	0.001	90	90	90
Ag/BEA	0.002	0.007	0.001	90	90	90
Pd/BEA	0.015	0.012	0.007	82	134	178
ZSM-5	0.000	0.000	0.000	90	90	90
Ag/ZSM-5	0.003	0.007	0.000	90	90	90
Pd/ZSM-5	0.010	0.016	0.007	84	188	294
SSZ-13	0.002	0.007	0.001	91	91	198
Ag/SSZ-13	0.002	0.004	0.002	88	88	191
Pd/SSZ-13	0.028	0.028	0.008	89	224	264

2.3. Hydrothermal Aging

After fully evaluating all the samples, five of the most promising zeolites were hydrothermally aged to investigate their durability. BEA, Pd/BEA, ZSM-5, Pd/ZSM-5, and Pd/SSZ-13 were heated to 800 °C for 50 h and re-evaluated following the same protocols as before. Figure 6 shows the HC metrics for both storage and release with the values listed in Table 3. The amount of deactivation is minimal on storage, as the change is less than 10%. The release temperatures for HCs are also similarly unchanged, as the T10s, T50s, and T90s are generally within a couple degrees of each other. The Pd/ZSM-5 sample did result in a higher release temperature, as the T90 increased from 195 to 216 °C, suggesting its oxidation capability diminished after aging. This is supported by the closer match of storage and release quantities, 4.7 and 4.5 (mmols C_1/g_{cat}). However, Pd/BEA maintained a large discrepancy in storage and release values as greater than 50% of the stored HCs are converted during release. In deciding which one of these samples would offer the best HCT functionality, it is clear that each of these hydrothermally aged samples would offer significant HCT capacity. The release profile of unexchanged BEA is slightly more favorable, since ~50% of the stored HCs are released above 200 °C, compared to 185 °C for ZSM-5. If Pd is going to be used for HCTs, Pd/BEA offers significant durability, and although Pd does not aid in the storage capacity, its oxidation capability is valuable with the ability to oxidize over 50% of the stored HCs even after hydrothermal aging.

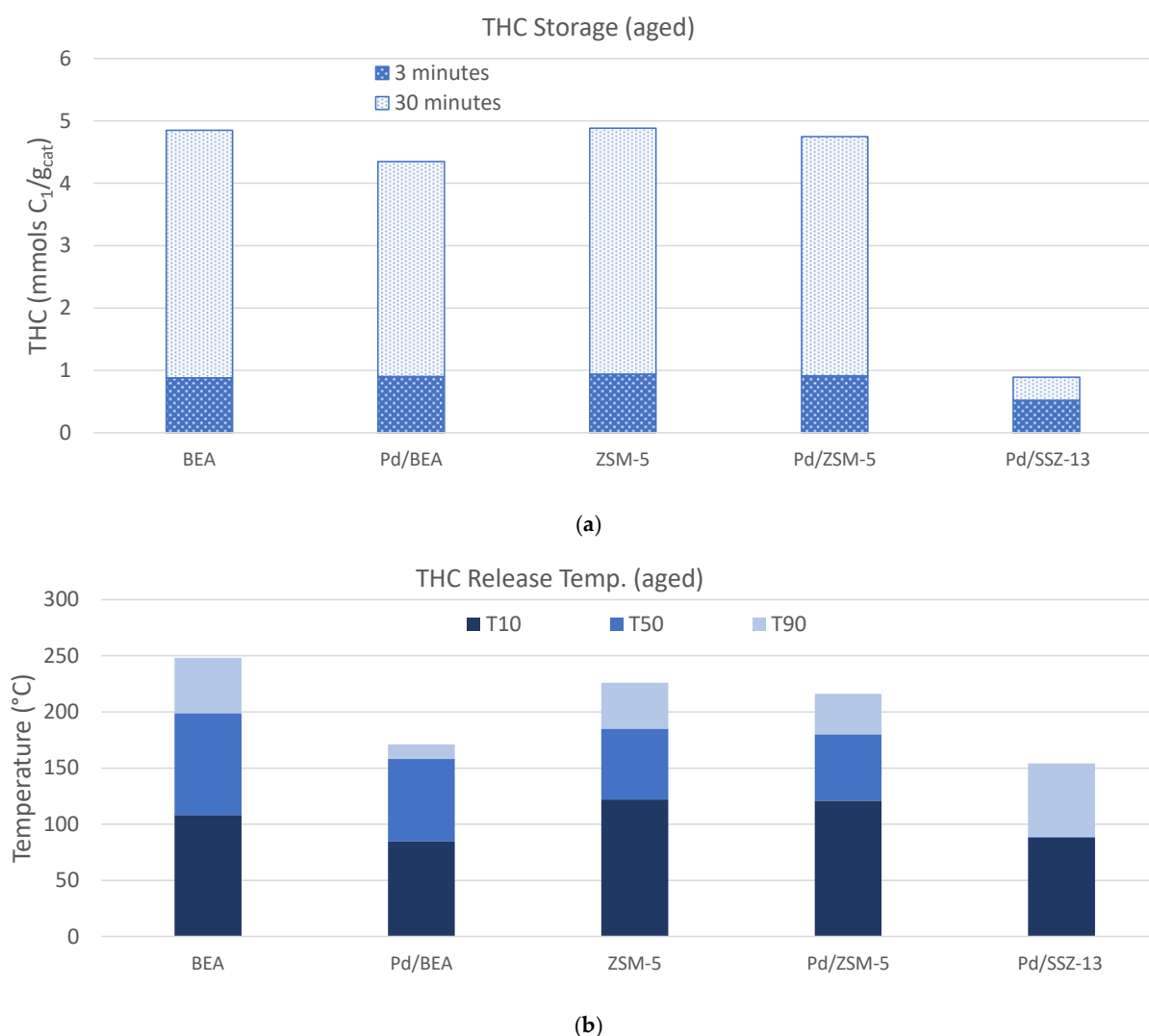


Figure 6. Following hydrothermal aging at 800 °C for 50 h (a) THC adsorption after 3 (■) and 30 (▨) minutes for each of the materials studied, and (b) the temperature where 10% (T10, ■), 50% (T50, ■), or 90% (T90, ■) of THC is released.

Table 3. THC storage values (mmol/g_{cat}) for hydrothermally aged samples; THCs are reported on a C₁ basis. The temperature where 10% (T10), 50% (T50), or 90% (T90) of THC is released is also shown.

LTC-D (Storage) Aged Zeolite	NOx Storage (mmols C ₁ /g _{cat})		NOx Release (mmols C ₁ /g _{cat})	Release Temperature		
	3 min	30 min	15 min	T10 (°C)	T50 (°C)	T90 (°C)
BEA	0.9	4.8	4.9	108	199	248
Pd/BEA	0.9	4.3	2.1	85	158	171
ZSM-5	0.9	4.9	4.8	122	185	226
Pd/ZSM-5	0.9	4.7	4.5	121	180	216
Pd/SSZ-13	0.5	0.9	0.5	88	89	154

The NOx storage behavior was notably different after hydrothermally aging. Figure 7 shows the NOx storage and release metrics for the five aged samples with the values shown in Table 4. From these results it is clear only the Pd/SSZ-13 maintains significant NOx storage capacity; in fact, both the storage capacity and release characteristics improve after aging. The storage increased from 0.028 to 0.036 mmols NO_x/g_{cat}, and the T50 increased from 224 to 262 °C. Pd/BEA is the only other sample to show storage, but all of the NOx is released before 150 °C. All these results continue to reinforce that Pd/SSZ-13 is the only viable option for PNA amongst the samples studied here.

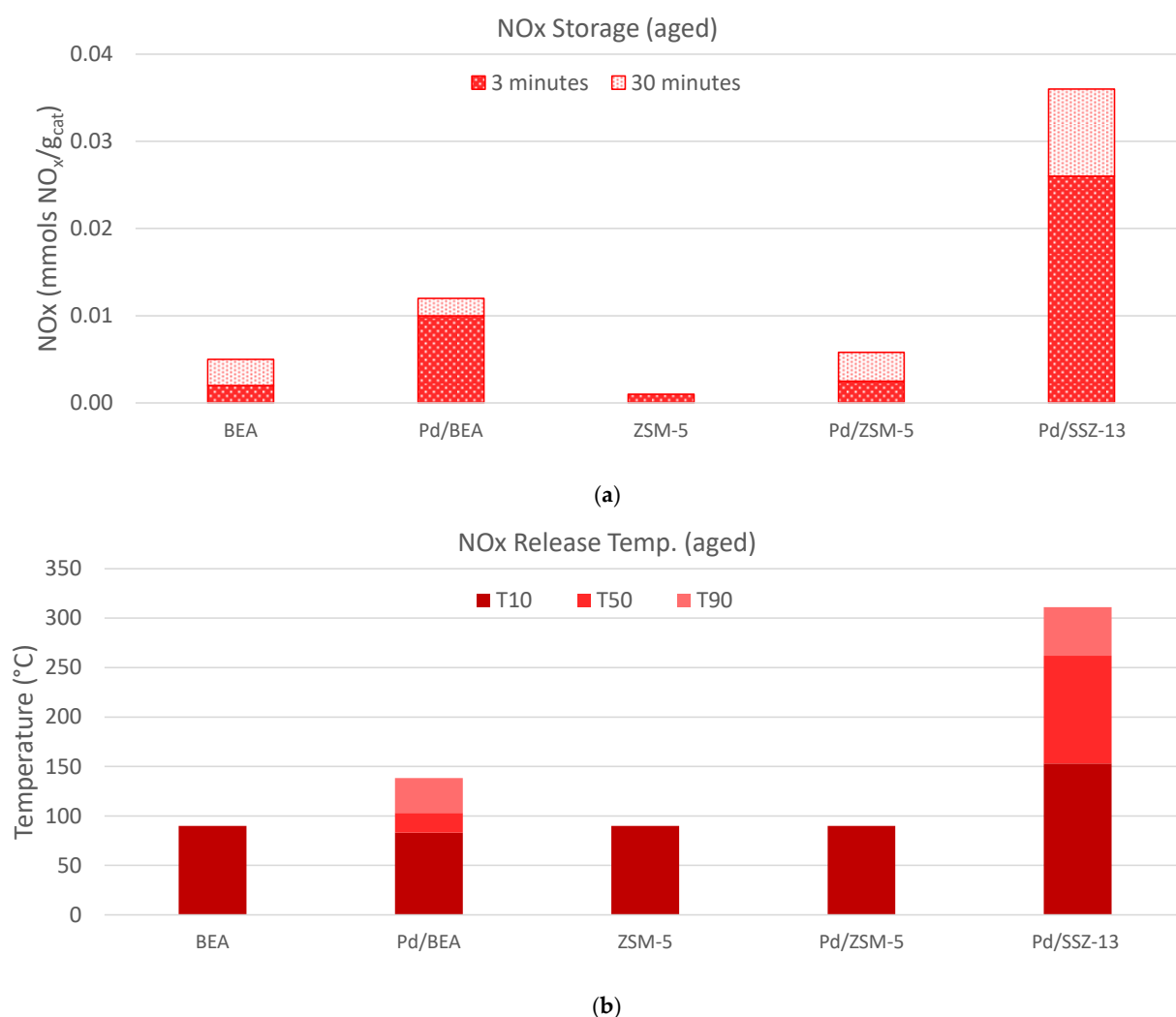


Figure 7. Following hydrothermal aging at 800 °C for 50 h (a) NO_x adsorption after 3 (■) and 30 (▨) minutes for each of the materials studied, and (b) the temperature where 10% (T10, ■), 50% (T50, ■), or 90% (T90, ■) of the NO_x is released.

Table 4. NO_x storage values (mmol/g_{cat}) for hydrothermally aged samples. The total amount of observed NO_x released during the first 15 min of the ramp, and the temperature where 10% (T10), 50% (T50), or 90% (T90) of NO_x is released is also shown.

LTC-D (Storage) Aged Zeolite	Storage (mmols NO _x /g _{cat})		Release (mmols NO _x /g _{cat}) 15 min	Release Temperature		
	3 min	30 min		T10 (°C)	T50 (°C)	T90 (°C)
BEA	0.002	0.005	0.002	90	90	90
Pd/BEA	0.010	0.012	0.004	83	103	138
ZSM-5	0.001	0.001	0.000	90	90	90
Pd/ZSM-5	0.003	0.006	0.000	90	90	90
Pd/SSZ-13	0.026	0.036	0.021	153	262	311

3. Experimental

3.1. Synthesis of Ion-Exchanged Zeolites

The traps studied here were synthesized by ion-exchange as reported previously [40]. Briefly, commercial BEA (CP814E)-Si/Al = 12.5 and ZSM-5 (CBV 3024E)-Si/Al = 15 zeolites were ion-exchanged with 75 mL of a 0.2 M AgNO₃ and 51 mL of a 9.4 mM Pd(NH₃)₄(NO₃)₂ stock solution at 60 °C and 80 °C for 24 h, respectively. Prior to ion-exchange the NH₄-form zeolites (as purchased from Zeolyst) were converted to their H-form by calcination at 500 °C for 2 h in static air. Single ionic exchange of Ag and Pd with BEA and ZSM-5 zeolites led to the synthesis of 1 wt.% Ag/BEA, 1 wt.% Ag/ZSM-5, 1 wt.% Pd/BEA and 1 wt.% Pd/ZSM-5 catalysts. The samples were filtered, washed with DI water, dried at 100 °C for 8 h and calcined in air at 500 °C for 2 h before further evaluation. For Pd/SSZ-13, an aqueous solution of Pd(NO₃)₂·2H₂O (0.037 mM, 10 mL) was added dropwise to the NH₄-SSZ-13-Si/Al = 15 suspension (3.960 g in 50 mL water; 250 RPM stirring) at 80 °C for 20 h. Filtered powder was calcined in air at 500 °C for 5 h. All samples were pelletized to 250–500 μm prior to evaluation. ICP was performed on several of the metal-exchanged materials in this study, and the metal loadings ranged from 0.97–1.07 wt.%, which is in good agreement with the expected value of 1 wt.%.

3.2. Trapping Characterization

Characterization of HC and NO_x trapping was conducted utilizing a storage protocol developed by the U.S. DRIVE Advanced Combustion and Emissions Control Technical Team [38,39]. Quartz wool and 100 mg of trapping material were loaded into an 8 mm diameter quartz reactor U-tube to create a plug-flow bed with one K-type thermocouple placed at the center of the bed and another K-type thermocouple approximately 1 cm above the bed to record bed and inlet temperatures, respectively. A visual description of the storage and release characterization is given in Figure 8. All materials were degreened in [O₂] = 12%, [CO₂] = 6%, and [H₂O] = 6% with Ar balance for 4 h at 700 °C prior to evaluation and the gas flow was normalized to 200 L·g⁻¹ h⁻¹. Water was introduced into the system via a bubbler set to 50.6 °C with heated lines to maintain vapor phase. Decane and toluene were introduced to the reactor similarly via a bubbler at 5 °C. Instrument response time baselines were determined through the reactor bypass by introduction of reactant gasses for 30 min via a 4-way switching valve. NO_x concentrations were determined by NO_x chemiluminescence analyzer (CLD 822 CM hr; Ecophysics, Dürnten, Switzerland) and the THC concentrations were determined by FID (flame ionization detector, California Analytical HFID-700, Orange, CA, USA) and reported on a C₁ basis. As needed, individual HC species were determined by mass spectrometer (Stanford Research Systems RGA 100, Sunnyvale, CA, USA) using m/z = 26, 57, and 91 for ethylene (C₂H₄), decane (C₁₀H₂₂), and toluene (C₇H₈), respectively.

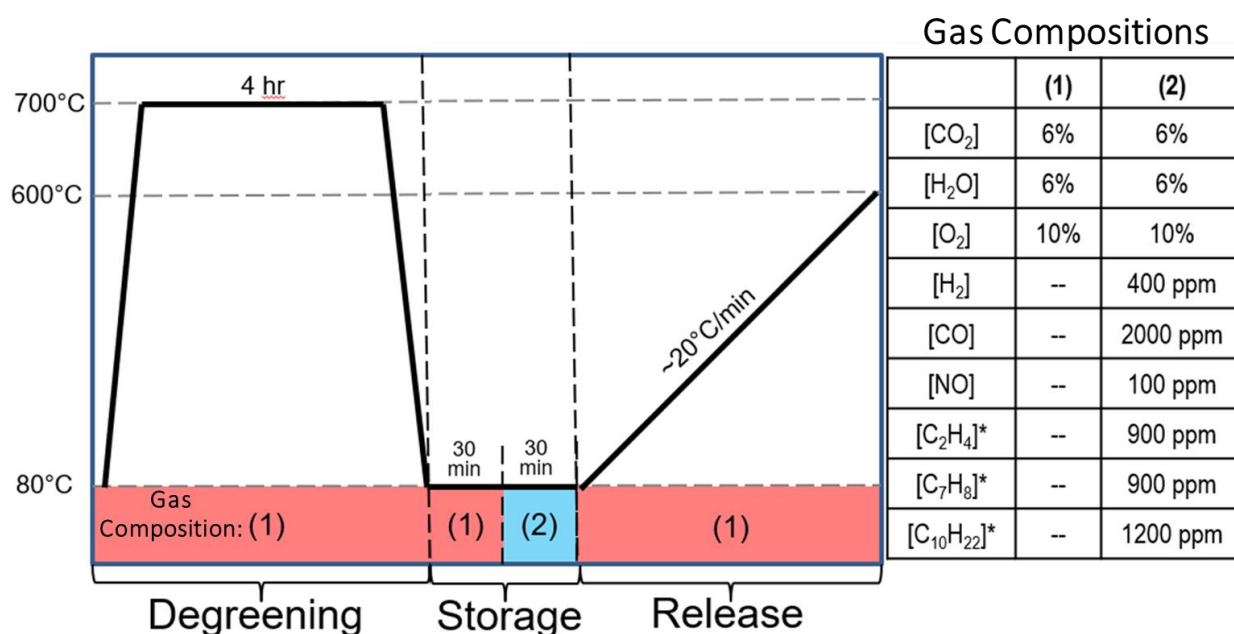


Figure 8. Storage and release characterization protocol (left) and gas concentrations (right). *—hydrocarbons are listed on a C₁ basis.

Storage and release were characterized sequentially by 30 min exposure of reactant gasses at 80 °C after which the temperature was ramped at 20 °C/min to a maximum temperature of 600 °C in the presence of the O₂, CO₂, and H₂O (Ar balance). Calculation of total reactant storage values and efficiencies were accomplished by subtraction of measured reactor outlet gas concentrations from the baseline, beginning and ending with the moment of valve switching. It should be noted the baseline is measured in the bypass line of the reactor. Release values were calculated by a similar comparison of baseline and reactor values during the 26 min temperature ramp and efficiencies are reported as a percentage of reactant stored. This storage/release procedure was repeated 3 times for each sample and then averaged.

Following the degreened evaluations of the samples, the most promising materials were hydrothermally aged at 800 °C for 50 h in [O₂] = 12%, [CO₂] = 6%, and [H₂O] = 6% with Ar balance. These samples were then re-evaluated according to the procedure outlined above. According to the low-temperature storage protocol [38,39], this time and temperature is intended to stress the materials to a similar level that would be expected at the end of their full-useful-life.

4. Conclusions

Overall, these samples show significant capability to perform both HCT and PNA functionalities. The presence of Ag or Pd does not universally result in increased HC storage, but Pd and its excellent oxidation reactivity aids in the conversion of the released HCs directly on the HCT. The pores of SSZ-13 are too small to store significant quantities of HCs, and thus BEA and ZSM-5 are preferred for HCTs. Pd is crucial for the adsorption of NO_x, and under these gas mixtures, Pd/SSZ-13 provides the best storage and release characteristics. Hydrothermal aging largely supports these results with minimal storage losses observed for BEA, Pd/BEA, ZSM-5, Pd/ZSM-5, and Pd/SSZ-13. Only Pd/BEA maintained its HC oxidation reactivity after aging. Pd/SSZ-13 is clearly the only sample evaluated to illustrate reasonable PNA behavior after aging, and in fact its storage capacity increased while its release temperature showed improved characteristics with greater than 50% of the stored NO_x being released above 250 °C.

Author Contributions: Conceptualization, T.J.T.; Data curation, T.J.T., A.J.B., P.K. and E.A.K.; Formal analysis, T.J.T. and J.-S.C.; Funding acquisition, T.J.T.; Investigation, T.J.T.; Methodology, T.J.T.; Project administration, T.J.T.; Supervision, T.J.T.; Writing—original draft, T.J.T. and A.J.B.; Writing—review and editing, T.J.T., P.K., E.A.K. and J.-S.C. All authors have read and agreed to the published version of the manuscript.

Funding: Funding for this work was provided by the U.S. Department of Energy’s Vehicle Technologies Office (VTO). The authors greatly appreciate support from Ken Howden, Siddiq Khan, and Gurpreet Singh at VTO.

Data Availability Statement: The data presented in this study are available on request from the corresponding author.

Acknowledgments: This manuscript has been authored by UT-Battelle, LLC, under Contract No. DE-AC0500OR22725 with the U.S. Department of Energy. The publisher, by accepting the article for publication, acknowledges that the United States Government retains a non-exclusive, paid-up, irrevocable, worldwide license to publish or reproduce the published form of this manuscript, or allow others to do so, for the United States Government purposes. The Department of Energy will provide public access to these results of federally sponsored research in accordance with the DOE Public Access Plan (<http://energy.gov/downloads/doe-public-access-plan>, accessed on 29 March 2021).

Conflicts of Interest: The authors declare no conflict of interest.

References

1. Dürnholtz, M.; Eifler, G.; Endres, H. *Exhaust-Gas Recirculation—A Measure to Reduce Exhaust Emissions of DI Diesel Engines*; No. 920725; SAE Technical Paper; SAE International: Warrendale, PA, USA, 1992. [CrossRef]
2. Johnson, T.V. Review of Diesel Emissions and Control. *Int. J. Engine Res.* **2009**, *10*, 275–285. [CrossRef]
3. Kyriakidou, E.A.; Toops, T.J.; Choi, J.-S.; Lance, M.J.; Parks, J.E., II. Exhaust Treatment Catalysts with Enhanced Hydrothermal Stability and Low-Temperature Activity. U.S. Patent 10,427,137 B2, 1 October 2019.
4. Wong, A.P.; Kyriakidou, E.A.; Toops, T.J.; Regalbuto, J.R. The Catalytic Behavior of Precisely Synthesized Pt-Pd Bimetallic Catalysts for Use as Diesel Oxidation Catalysts. *Catal. Today* **2016**, *267*, 145–156. [CrossRef]
5. Kim, M.-Y.; Kyriakidou, E.A.; Choi, J.-S.; Toops, T.J.; Binder, A.J.; Thomas, C.; Parks, J.E., II; Schwartz, V.; Chen, J.; Hensley, D.K. Enhancing Low-Temperature Activity and Durability of Pd-based Diesel Oxidation Catalysts Using ZrO₂ Supports. *Appl. Catal. B Environ.* **2016**, *187*, 181–194. [CrossRef]
6. Hoang, S.; Guo, Y.; Binder, A.; Tang, W.; Wang, S.; Liu, J.; Huan, T.; Lu, X.; Wang, Y.; Ding, Y.; et al. Activating Low-Temperature Diesel Oxidation by Single-Atom Pt on TiO₂ Nanowire Array. *Nat. Commun.* **2020**, *11*, 1–10.
7. Wang, A.; Olsson, L. The Impact of Automotive Catalysis on the United Nations Sustainable Development Goals. *Nat. Catal.* **2019**, *2*, 566–570. [CrossRef]
8. Johnson, T.V. Diesel Emissions in Review. *SAE Int. J. Engines* **2011**, *4*, 143–157. [CrossRef]
9. Zelinsky, R.; Epling, W. Effects of Multicomponent Hydrocarbon Feed on Hydrocarbon Adsorption—Desorption and Oxidation Light-Off Behavior on a Pd/BEA Hydrocarbon Trap. *Catal. Lett.* **2019**, *149*, 3194–3202. [CrossRef]
10. Beale, A.M.; Gao, F.; Lezcano-Gonzalez, I.; Peden, C.H.F.; Szanyi, J. Recent Advances in Automotive Catalysis for NO_x Emission Control by Small-Pore Microporous Materials. *Chem. Soc. Rev.* **2015**, *44*, 7371–7405. [CrossRef]
11. Naseri, M.; Aydin, C.; Mulla, S.; Conway, R.; Chatterjee, S. Development of Emission Control Systems to Enable High NO_x Conversion on Heavy Duty Diesel Engines. *SAE Int. J. Engines* **2015**, *8*, 1144–1151. [CrossRef]
12. Squaiella, L.L.F.; Martins, C.A.; Pedro, T.L. Strategies for Emission Control in Diesel Engine to Meet Euro VI. *Fuel* **2013**, *104*, 183–193. [CrossRef]
13. Lao, C.T.; Akroyd, J.; Eaves, N.; Smith, A.; Morgan, N.; Nurkowski, D.; Bhave, A.; Kraft, M. Investigation of the Impact of the Configuration of Exhaust After-Treatment System for Diesel Engines. *Appl. Energy* **2020**, *267*, 114844. [CrossRef]
14. Lyu, M.; Bao, X.; Zhu, R.; Matthews, R. State-of-the-Art Outlook for Light-Duty Vehicle Emission Control Standards and Technologies in China. *Clean Technol. Environ. Policy* **2020**, *22*, 757–771. [CrossRef]
15. Weilenmann, M.; Favez, J.-Y.; Alvarez, R. Cold-Start Emissions of Modern Passenger Cars at Different Low Ambient Temperatures and Their Evolution over Vehicle Legislation Categories. *Atmos. Environ.* **2009**, *43*, 2419–2429. [CrossRef]
16. Iliyas, A.; Zahedi-Niaki, M.H.; Eić, M.; Kaliaguine, S. Control of Hydrocarbon Cold-Start Emissions: A Search for Potential Adsorbents. *Microporous Mesoporous Mater.* **2007**, *102*, 171–177. [CrossRef]
17. Lee, J.; Theis, J.R.; Kyriakidou, E.A. Vehicle Emissions Trapping Materials: Successes, Challenges, and the Path Forward. *Appl. Catal. B Environ.* **2019**, *243*, 397–414. [CrossRef]
18. Curran, S.; Prikhodko, V.; Cho, K.; Sluder, C.S.; Parks, J.; Wagner, R.; Kokjohn, S.; Reitz, R.D. *In-Cylinder Fuel Blending of Gasoline/Diesel for Improved Efficiency and Lowest Possible Emissions on a Multi-Cylinder Light-Duty Diesel Engine*; No. 2010-01-2206; SAE Technical Paper; SAE International: Warrendale, PA, USA, 2010.

19. Zheng, M.; Asad, U.; Graham, T.; Reader, Y.T.; Wang, M. Energy Efficiency Improvement Strategies for a Diesel Engine in Low-Temperature Combustion. *Int. J. Energy Res.* **2009**, *33*, 8–28. [CrossRef]
20. Zammit, M.; DiMaggio, C.; Kim, C.; Lambert, C.; Muntean, G.; Peden, C.; Parks, J.; Howden, K. Future Automotive Aftertreatment Solutions: The 150 °C Challenge Workshop Report. Available online: https://cleers.org/wp-content/uploads/2012_The_150C_Challenge_Workshop_Report.pdf (accessed on 29 March 2021).
21. Environmental Protection Agency, U.S. EPA-420-F-13-016a; U. S. Environmental Protection Agency: Washington, DC, USA, 2013; pp. 1–4.
22. Environmental Protection Agency, U.S.; Department of Transportation, National Highway Traffic Safety Administration. 2017 and Later Model Year Light-Duty Vehicle Greenhouse Gas Emissions and Corporate Average Fuel Economy Standards. *Fed. Regist.* **2012**, *77*, 62623–63200.
23. Sarshar, Z.; Zahedi-Niaki, M.H.; Huang, Q.; Eić, M.; Kaliaguine, S. MTW Zeolites for Reducing Cold-Start Emissions of Automotive Exhaust. *Appl. Catal. B Environ.* **2009**, *87*, 37–45. [CrossRef]
24. Burke, N.R.; Trimm, D.L.; Howe, R.F. The Effect of Silica:Alumina Ratio and Hydrothermal Ageing on the Adsorption Characteristics of BEA Zeolites for Cold Start Emission Control. *Appl. Catal. B Environ.* **2003**, *46*, 97–104. [CrossRef]
25. Huuhtanen, M.; Rahkamaa-Tolonen, K.; Maunula, T.; Keiski, R.L. Pt-Loaded Zeolites for Reducing Exhaust Gas Emissions at Low Temperatures and in Lean Conditions. *Catal. Today* **2005**, *100*, 321–325. [CrossRef]
26. López, J.M.; Navarro, M.V.; García, T.; Murillo, R.; Mastral, A.M.; Varela-Gandía, F.J.; Lozano-Castelló, D.; Bueno-López, A.; Cazorla-Amorós, D. Screening of Different Zeolites and Silicoaluminophosphates for the Retention of Propene Under Cold Start Conditions. *Microporous Mesoporous Mater.* **2010**, *130*, 239–247. [CrossRef]
27. Kim, D.J.; Kim, J.W.; Yie, J.E.; Moon, H. Temperature-Programmed Adsorption and Characteristics of Honeycomb Hydrocarbon Adsorbers. *Ind. Eng. Chem. Res.* **2002**, *41*, 6589–6592. [CrossRef]
28. Kim, H.; Jang, E.; Jeong, Y.; Kim, J.; Kang, C.Y.; Kim, C.H.; Baik, H.; Lee, K.-Y.; Choi, J. On the Synthesis of a Hierarchically-Structured ZSM-5 Zeolite and the Effect of its Physicochemical Properties with Cu Impregnation on Cold-Start Hydrocarbon Trap Performance. *Catal. Today* **2018**, *314*, 78–93. [CrossRef]
29. Westermann, A.; Azambre, B.; Chebbi, M.; Koch, A. Modification of Y Faujasite Zeolites for the Trapping and Elimination of a Propene-Toluene-Decane Mixture in the Context of Cold-Start. *Microporous Mesoporous Mater.* **2016**, *230*, 76–88. [CrossRef]
30. Azambre, B.; Westermann, A.; Fiqueneisel, G.; Can, F.; Comparot, J.D. Adsorption and Desorption of a Model Hydrocarbon Mixture Over HY Zeolite under Dry and Wet Conditions. *J. Phys. Chem. C* **2015**, *119*, 315–331. [CrossRef]
31. Zheng, Y.; Kovarik, L.; Mark, H.; Engelhard, Y.W.; Wang, Y.; Gao, F.; Szanyi, J. Low-Temperature Pd/Zeolite Passive NOx Adsorbers: Structure, Performance, and Adsorption Chemistry. *J. Phys. Chem. C* **2017**, *121*, 15793–15803. [CrossRef]
32. Yu, Q.; Chen, X.; Bhat, A.; Tang, X.; Yi, H.; Lin, X.; Schwank, J.W. Activation of Passive NOx Adsorbers by Pretreatment with Reaction Gas Mixture. *Chem. Eng. J.* **2020**, *399*, 125727. [CrossRef]
33. Ryou, Y.; Lee, J.; Lee, H.; Kim, C.H.; Kim, D.H. Effect of Various Activation Conditions on the Low Temperature NO Adsorption Performance of Pd/SSZ-13 Passive NOx Adsorber. *Catal. Today* **2019**, *320*, 175–180. [CrossRef]
34. Malamis, S.A.; Harold, M.P.; Epling, W.S. Coupled NO and C3H6 Trapping, Release and Conversion on Pd/BEA: Evaluation of the Lean Hydrocarbon NOx Trap. *Ind. Eng. Chem. Res.* **2019**, *58*, 22912–22923. [CrossRef]
35. Chen, H.-Y.; Mulla, S.; Weigert, E.; Camm, K.; Ballinger, T.; Cox, J.; Blakeman, P. Old Start Concept (CSCTM): A Novel Catalyst for Cold Start Emission Control. *SAE Int. J. Fuels Lubr.* **2013**, *6*, 372–381. [CrossRef]
36. Lupescu, J.; Chanko, T.; Richert, J.; DeVries, J. Treatment of Vehicle Emissions from the Combustion of E85 and Gasoline with Catalyzed Hydrocarbon Traps. *SAE Int. J. Fuels Lubr.* **2009**, *2*, 485–496. [CrossRef]
37. Nunan, J.; Lupescu, J.; Denison, G.; Ball, D.; Moser, D. HC Traps for Gasoline and Ethanol Applications. *SAE Int. J. Fuels Lubr.* **2013**, *6*, 430–449. [CrossRef]
38. Aftertreatment Protocols for Catalyst Characterization and Performance Evaluation: Low-Temperature Storage Catalyst Test Protocol. Available online: https://cleers.org/wp-content/uploads/2018/03/2018_LTAT_Low-Temperature-Storage-Protocol.pdf (accessed on 29 March 2021).
39. Kenneth, G.; Rappé, C.D.; Josh, A.; Pihl, J.R.; Theis, S.; Oh, H.; Galen, B.; Fisher, J.P.; Vencon, G.; Easterling, M.Y.; et al. Aftertreatment Protocols for Catalyst Characterization and Performance Evaluation: Low-Temperature Oxidation, Storage, Three-Way, and NH₃-SCR Catalyst Test Protocols. *Emiss. Control Sci. Technol.* **2019**, *5*, 183–214. [CrossRef]
40. Kyriakidou, E.A.; Lee, J.; Choi, J.-S.; Lance, M.; Toops, T.J. A Comparative Study of Silver- and Palladium-Exchanged Zeolites in Propylene and Nitrogen Oxide Adsorption and Desorption for Cold-Start Applications. *Catal. Today* **2020**. [CrossRef]
41. Chen, H.-Y.; Collier, J.E.; Liu, D.; Mantarosie, L.; Durán-Martín, D.; Novák, V.; Rajaram, R.R.; Tompsett, D. Low Temperature NO Storage of Zeolite Supported Pd for Low Temperature Diesel Engine Emission Control. *Catal. Lett.* **2016**, *146*, 1706–1711. [CrossRef]
42. Westermann, A.; Azambre, B.; Fiqueneisel, G.; Da Costa, P.; Can, F. Evolution of Unburnt Hydrocarbons Under ‘Cold-Start’ Conditions from Adsorption/Desorption to Conversion: On the Screening of Zeolitic Materials. *Appl. Catal. B* **2014**, *158–159*, 48–59. [CrossRef]
43. Kang, S.B.; Kalamaras, C.; Balakotaiah, V.; Epling, W. Hydrocarbon Trapping over Ag-Beta Zeolite for Cold-Start Emission Control. *Catal. Lett.* **2017**, *147*, 1355–1362. [CrossRef]

44. Khivantsev, K.; Jaegers, N.R.; Kovarik, L.; Hanson, J.C.; Tao, F.; Tang, Y.; Zhang, X.; Koleva, I.Z.; Aleksandrov, H.A.; Vayssilov, G.N.; et al. Achieving Atomic Dispersion of Highly Loaded Transition Metals in Small-Pore Zeolite SSZ-13: High-Capacity and High Efficiency Low Temperature CO and Passive NO_x Adsorbers. *Angew. Chem.* **2018**, *57*, 16672–16677. [[CrossRef](#)]
45. Ryou, Y.; Lee, J.; Cho, S.J.; Lee, H.; Kim, C.H.; Kim, D.H. Activation of Pd/SSZ-13 Catalyst by Hydrothermal Aging Treatment in Passive NO Adsorption Performance at Low Temperature for Cold Start Application. *Appl. Catal. B* **2017**, *212*, 140–149. [[CrossRef](#)]
46. Lee, J.; Ryou, Y.S.; Hwang, S.; Kim, Y.; Cho, S.J.; Lee, H.; Kim, C.H.; Kim, D.H. Comparative Study of the Mobility of Pd Species in SSZ-13 and ZSM-5, and its Implication for their Activity as Passive NO_x Adsorber (PNAs) after Hydro-Thermal Aging. *Catal. Sci. Technol.* **2019**, *9*, 163–173. [[CrossRef](#)]
47. Ball, D.; Zammit, M.; Wuttke, J.; Buitrago, C. Investigation of LEV-III Aftertreatment Designs. *SAE Int. J. Fuels Lubr.* **2011**, *4*, 1–8. [[CrossRef](#)]
48. Gao, Z.; Kim, M.-Y.; Choi, J.-S.; Daw, C.S.; Parks, J.E., II; Smith, D.E. Cold-Start Emissions Control in Hybrid Vehicles Equipped with a Passive Adsorber for Hydrocarbons and Nitrogen Oxides. *J. Automob. Eng.* **2012**, *226*, 1396–1407. [[CrossRef](#)]
49. McLeary, E.E.; Jansen, J.C.; Kapteijn, F. Zeolite Based Films, Membranes and Membrane Reactors: Progress and Prospects. *Microporous Mesoporous Mater.* **2006**, *90*, 198–220. [[CrossRef](#)]
50. Li, Y.; Li, L.; Yu, J. Applications of Zeolites in Sustainable Chemistry. *Chem* **2017**, *3*, 928–949. [[CrossRef](#)]
51. Jonsson, R.; Woo, J.; Skoglundh, M.; Olsson, L. Zeolite Beta Doped with La, Fe, and Pd as a Hydrocarbon Trap. *Catalysts* **2020**, *10*, 173. [[CrossRef](#)]
52. Park, J.H.; Park, S.J.; Ahn, H.A.; Nam, I.S.; Yeo, G.K.; Kil, J.K.; Youn, Y.K. Promising Zeolite-Type Hydrocarbon Trap Catalyst by a Knowledge-Based Combinatorial Approach. *Microporous Mesoporous Mater.* **2009**, *117*, 178–184. [[CrossRef](#)]
53. Schaber, P.M.; Colson, J.; Higgins, S.; Thielen, D.; Anspach, B.; Brauer, J. Thermal Decomposition (Pyrolysis) of Urea in an Open Reaction Vessel. *Thermochim. Acta* **2004**, *424*, 131–142. [[CrossRef](#)]
54. Xu, M.; Wang, J.; Yu, T.; Wang, J.; Shen, M. New Insight into Cu/SAPO-34 Preparation Procedure: Impact of NH₄-SAPO-34 on the Structure and Cu Distribution in Cu-SAPO-34 NH₃-SCR Catalysts. *Appl. Catal. B Environ.* **2018**, *220*, 161–170. [[CrossRef](#)]
55. Rahkamaa-Tolonen, K.; Maunula, T.; Lomma, M.; Huuhtanen, M.; Keiski, R.L. The Effect of NO₂ on the Activity of Fresh and Aged Zeolite Catalysts in the NH₃-SCR Reaction. *Catal. Today* **2005**, *100*, 217–222. [[CrossRef](#)]
56. Konstantin, K.; Feng, G.; Libor, K.; Yong, W.; János, S. Molecular Level Understanding of How Oxygen and Carbon Monoxide Improve NO_x Storage in Palladium/SSZ-13 Passive NO_x Adsorbers: The Role of NO⁺ and Pd(II)(CO)(NO) Species. *J. Phys. Chem. C* **2018**, *122*, 10820–10827. [[CrossRef](#)]
57. Yongwoo, K.; Sungha, H.; Jaeha, L.; YoungSeok, R.; Hyokyoun, L.; Chang, H.K.; Do Heui, K. Comparison of NO_x Adsorption/Desorption Behaviors over Pd/CeO₂ and Pd/SSZ-13 as Passive NO_x Adsorbers for Cold Start Application. *Emiss. Control Sci. Technol.* **2019**, *5*, 172–182. [[CrossRef](#)]